www.czasopisma.pan.pl PAN POLSKA AKADEMIA NAUK www.journals.pan.pl

A R C H I V E S O F M E T A L L U R G Y A N D M A T E R I A L S

Volume 60 2015 Issue 3

DOI: 10.1515/amm-2015-0389

T. LIPIŃSKI*#

EFFECT OF THE SPACING BETWEEN SUBMICROSCOPIC OXIDE IMPURITIES ON THE FATIGUE STRENGTH OF STRUCTURAL STEEL

WPŁYW ODLEGŁOŚCI POMIĘDZY SUBMIKROSKOPOWYMI ZANIECZYSZCZENIAMI TLENKOWYMI NA WYTRZYMAŁOŚĆ ZMĘCZENIOWĄ STALI KONSTRUKCYJNEJ

The article discusses the effect of distance between submicroscopic oxide impurities (up to 2 μm in size) on the fatigue resistance coefficient of structural steel during rotary bending. The study was performed on 21 heats produced in an industrial plant. Fourteen heats were produced in 140 ton electric furnaces, and 7 heats were performed in a 100 ton oxygen converter. All heats were desulfurized. Furthermore seven heats from electrical furnaces were refined with argon, and heats from the converter were subjected to vacuum circulation degassing.

Steel sections with a diameter of 18 mm were hardened from austenitizing by 30 minutes in temperature 880°C and tempered at a temperature of 200, 300, 400, 500 and 600°C. The experimental variants were compared in view of the applied melting technology and heat treatment options. The results were presented graphically and mathematically. The fatigue resistance coefficient of structural steel with the effect of spacing between submicroscopic oxide impurities was determined during rotary bending. The results revealed that fatigue resistance coefficient *k* is determined by the distance between submicroscopic non-metallic inclusions and tempering temperature.

Keywords: steel, structural steel, non-metallic inclusions, fatigue strength, oxide impurities, fatigue resistance coefficient, bending fatigue, bending pendulum

W pracy przedstawiono wyniki badań wpływu odległości pomiędzy submikroskopowymi zanieczyszczeniami tlenkowymi, o wielkości do 2 μm, na wskaźnik odporności na zmęczenie stali konstrukcyjnej przy zginaniu obrotowym. Badania prowadzono na 21 wytopach wyprodukowanych w warunkach przemysłowych. 14 wytopów wykonano w piecach elektrycznych o pojemności 140 ton i 7 wytopów w konwertorze tlenowym o pojemności 100 ton. Wszystkie wytopy poddawano odsiarczaniu. Dodatkowo 7 wytopów pochodzących z pieca elektrycznego poddawano rafinacji argonem, zaś wytopy z konwertora odgazowaniu próżniowemu.

Odcinki ze stali o średnicy 18 mm hartowano po austenityzowaniu w czasie 30 minut z temperatury 880°C i odpuszczano w temperaturach: 200, 300, 400, 500 lub 600°C. Warianty badań zestawiono uwzględniając technologię wytapiania stali opcje obróbki cieplnej. Wyniki przedstawiono w graficznej i matematycznej postaci uwzględniającej zależności wskaźnik odporności na zmęczenie przy obrotowym zginaniu z odległości pomiędzy submikroskopowymi zanieczyszczeniami. Wykazano, że wskaźnik odporności na zmęczenie *k* zależy od odległości pomiędzy submikroskopowymi wtrąceniami niemetalicznymi, oraz temperatury odpuszczania.

1. Introduction

The elements of various structures are exposed to variable loads [1]. Their fatigue strength and threshold stress levels have to be determined to optimize the designed structure. During laboratory tests, attempts are made to recreate the actual conditions that impact structural materials in moving machine parts. Such tests are conducted on both specimens and existing machine parts.

The strength of materials and machine parts is generally evaluated in destructive tests. Specimens that had been subjected to strength tests are no longer fit for use as structural components. A series of process algorithms have been developed to determine the strength properties of materials without causing structural damage. Those algorithms rely on non-destructive tests (NDT) such as ultrasound or radiological examinations. Processes that influence the structural properties of materials are modeled [2-3]. The strength of structural materials can also be assessed based

* UNIVERSITY OF WARMIA AND MAZURY IN OLSZTYN, THE FACULTY OF TECHNICAL SCIENCES, 11 OCZAPOWSKIEGO STR., 10-957 OLSZTYN, POLAND

Corresponding author: tomekl@uwm.edu.pl

on other tests that do not cause damage to the examined parts, such as hardness tests. Various indicators that support effective evaluation of the tensile strength of specific materials, subject to hardness, have been proposed in the literature ($R_m = c$ HV). Other correlations are used to estimate a material's fatigue strength based on its tensile strength ($z_{go} = e\ R_m$) [4]. However, both approaches (z_{go} and R_m) involve destructive tests. A better solution is to estimate fatigue strength (which is a costly and time-consuming test) based on a material's hardness, with the use of fatigue resistance coefficient k – the quotient of fatigue strength z_{go} and Vickers hardness HV (1).

$$k = \frac{z_{go}}{HV} \tag{1}$$

The mechanical properties and fatigue strength of structural materials should also be evaluated in view of crystallization conditions [5-11], the manufacturing process [12-15], microstructure [16,17], microsegregation [18-22] and the existing defects [23-25].

Real-life materials are characterized by numerous imperctions which result from manufacturing processes. Non-metallic inclusions are one of such defects [26-29]. The quantity and quality of non-metallic inclusions determine the mechanical properties and fatigue strength of materials [30,31]. The effects of microstructure, quantity and morphology of impurities and other parameters on fatigue strength have been extensively researched. Particular attention was paid to hard steels where non-metallic inclusions, mostly large defects observed on the surface, lower a material's strength under exposure to variable loads [32-35]. The effect of submicroscopic impurities on fatigue strength is much more difficult to analyze and is, therefore, less frequently investigated.

In a correctly performed metallurgical process, non-metallic inclusions in steel are randomly distributed, and their quantity can be described by the distance between inclusions λ, which was investigated in the present study.

2. Aim of the study and methods

The objective of this study was to determine changes in fatigue resistance coefficient k subject to the distance between non-metallic inclusions and variations in the microstructural characteristics of structural steel.

The tested material comprised steel manufactured in three different metallurgical processes. The resulting heats differed in purity and size of non-metallic inclusions. Heat treatments were selected to produce heats with different microstructure of steel, from hard microstructure of tempered martensite, through sorbitol to the ductile microstructure obtained by spheroidization.

In the first process, steel was melted in a 140-ton basic arc furnace. The study was performed on 21 heats produced in an industrial plant. The metal was tapped into a ladle, it was desulfurized and 7-ton ingots were uphill teemed. Billets with a square section of 100×100 mm were rolled with the use of conventional methods. As part of the second procedure. After tapping into a ladle, steel was additionally refined with argon. Gas was introduced through a porous brick, and the procedure was completed in 8-10 minutes. Steel was poured into moulds, and billets were rolled similarly as in the first method. In the third process, steel was melted in a 100-ton oxygen converter and deoxidized by vacuum. Steel was cast continuously and square 100×100 mm billets were rolled. Billet samples were collected to determine: chemical composition – the content of alloy constituents was estimated with the use of LECO analyzers an AFL FICA 31000 quantometer and conventional analytical methods, relative volume of non-metallic inclusions with the use of the extraction method, dimensions of impurities by inspecting metallographic specimens with the use of a Quantimet 720 video inspection microscope under 400× magnification. It was determined for a larger boundary value of 2 μm.

The number of particles range 2 μm and smaller was the difference between the number of all inclusions determined by chemical extraction and the number of inclusions measured by video method.

Analytical calculations were performed on the assumption that the quotient of the number of particles on the surface divided by the area of that surface was equal to the quotient of the number of particles in volume divided by that volume [36].

It in aim of qualification of fatigue proprieties from every melting was taken 51 sections. The sections possessing the shapes of cylinder about diameter 10 mm. Their main axes are directed to direction of plastic processing simultaneously. It thermal processing was subjected was in aim of differentiation of building of structural sample. It depended on hardening from austenitizing by 30 minutes in temperature 880°C after which it had followed quenching in water, for what was applied drawing. Tempering depended on warming by 120 minutes material in temperature 200, 300, 400, 500 or 600°C and cooling down on air.

The average chemical composition of the analyzed steel is presented in Table 1.

TABLE 1

Average chemical composition of the analyzed steel

C	Mn	Si	P	S	Cr	Ni	Mo	Cu	B
0.24	1.19	0.25	0.02	0.013	0.51	0.49	0,24	0.11	0.003

Fatigue strength was determined for all heats. Heat treatment was applied to evaluate the effect of hardening on the fatigue properties of the analyzed material, subject to the volume of fine non-metallic inclusions. The application of various heat treatment parameters led to the formation of different microstructures responsible for steel hardness values in the following range from 271 to 457 HV [28].

Examination was realized on calling out to rotatory curving machine about frequency of pendulum cycles: 6000 periods on minute. For basis was accepted was on fatigue defining endurance level 10^7 cycles. The level of fatigue-inducing load was

adapted to the strength properties of steel. Maximum load was set for steel tempered at a temperature of: 200°C – 650 MPa, from 300°C to 500°C – 600 MPa, 600°C – 540 MPa [13-16,27,28].

During the test, the applied load was gradually reduced in steps of 40 MPa (to support the determinations within the endurance limit). Load values were selected to produce 10^4-10^6 cycles characterizing endurance limits [1].

The arithmetic average impurities spacing each of the heats λ were calculated with the use of the below formula (2):

$$\lambda = \frac{2}{3}\bar{d}\left(\frac{1}{V_0} - 1\right) \tag{2}$$

where:

$\bar{d}$ – the average diameter of impurity, µm,

V_0 – the relative volume of submicroscopic impurities, %.

The general form of the mathematical model is presented by equation (3) and (4)

$$\lambda = a\, V_0 + b \tag{3}$$

or

$$k_{(\text{temp. tempered})} = a\,\lambda + b \tag{4}$$

where:

k – fatigue resistance coefficient,

λ – arithmetic average distance between submicroscopic oxide iurities (impurities spacing) for each of the heats, µm

V_0 – relative volume of non-metallic inclusions range 2 µm and smaller, vol. %.

a, b – coefficients of the equation

The significance of correlation coefficients r was determined on the basis of the critical value of the Student's t-distribution for a significance level $\alpha = 0.05$ and the number of degrees of freedom $f = n - 2$ by formula (5).

$$t = \frac{r}{\sqrt{\frac{1-r^2}{n-2}}} \tag{5}$$

The values of the diffusion coefficient z_{go} near the regression line were calculated with the use of the below formula (6):

$$\delta = 2s\sqrt{1-r^2} \tag{6}$$

where:

s – standard deviation,

r – correlation coefficient.

The values of the standard deviation s were calculated with the use of the below formula (7):

$$s = \sqrt{\frac{\sum\left(x-\bar{x}\right)^2}{\left(n-1\right)}} \tag{7}$$

where:

x – result of measurement,

$\bar{x}$ – arithmetic average of measurement results.

3. The results of investigations and their analysis

The arithmetic average impurities spacing each of the heats $\bar{\lambda}$. subject to volume of inclusions V_0 of steel is presented in Fig. 1, regression equation and correlation coefficient r at (8).

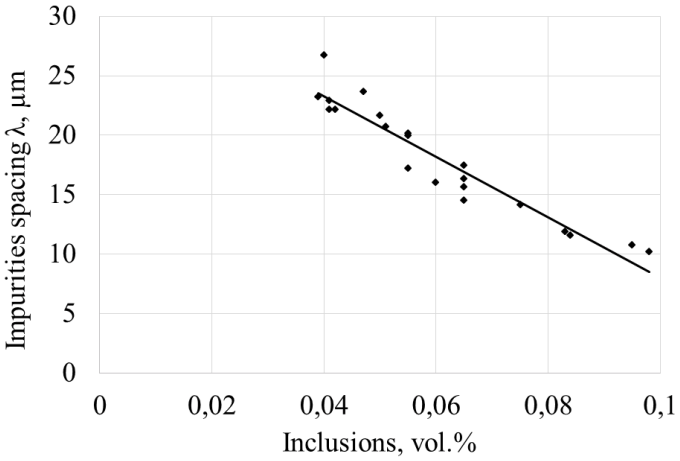

Fig. 1. Arithmetic average impurities spacing each of the heats l subject to volume of inclusions V_0

$$\lambda = -245.05\, V_0 + 33.418 \quad \text{and} \quad r = 0.9516 \tag{8}$$

Fatigue resistance coefficient k determined for bending fatigue strength of steel hardened and tempered at 200°C in dependence on arithmetic average distance between submicroscopic oxide impurities are presented in Fig. 2, regreson equation and correlation coefficient r at (9).

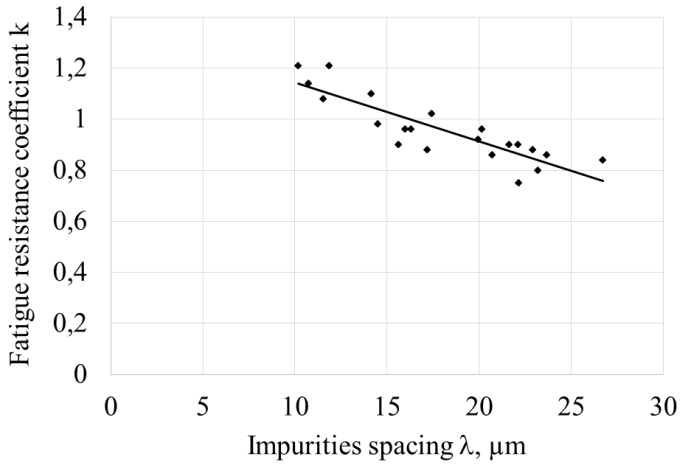

Fig. 2. Fatigue resistance coefficient k of steel hardened and tempered at 200°C subject to arithmetic average distance between submicroscopic oxide impurities (impurities spacing) λ

$$k_{(200)} = -0.0231\, l + 1.3737 \quad \text{and} \quad r = 0.8650 \tag{9}$$

Fatigue resistance coefficient k determined for bending fatigue strength of steel hardened and tempered at 300°C in dependence on arithmetic average distance between submicroscopic oxide impurities are presented in Fig. 3, regression equation and correlation coefficient r at (10).

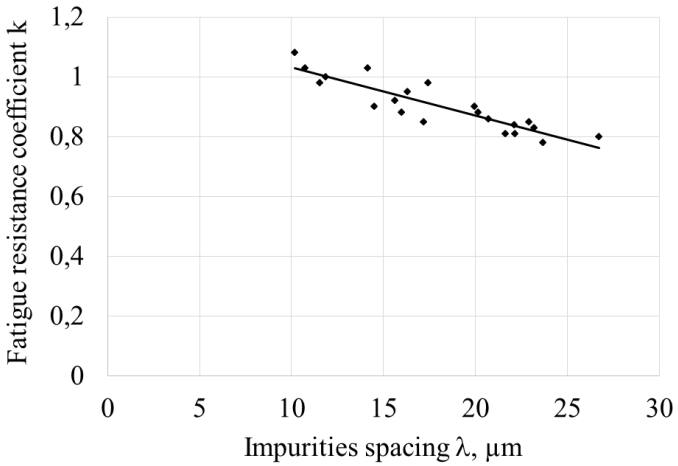

Fig. 3. Fatigue resistance coefficient k of steel hardened and tempered at 300°C subject to arithmetic average distance between submicroscopic oxide impurities (impurities spacing) λ

$$k_{(300)} = -0.0161\,\mathrm{l} + 1.193 \quad \text{and} \quad r = 0.8926 \qquad (10)$$

Fatigue resistance coefficient k determined for bending fatigue strength of steel hardened and tempered at 400°C in dependence on arithmetic average distance between submicroscopic oxide impurities are presented in Fig. 4, regression equation and correlation coefficient r at (11).

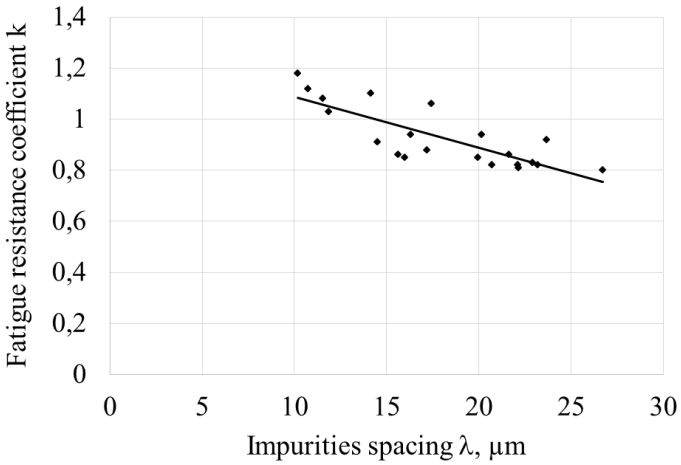

Fig. 4. Fatigue resistance coefficient k of steel hardened and tempered at 400°C subject to arithmetic average distance between submicroscopic oxide impurities (impurities spacing) λ

$$k_{(400)} = -0.02\,\mathrm{l} + 1.2878 \quad \text{and} \quad r = 0.8059 \qquad (11)$$

Fatigue resistance coefficient k determined for bending fatigue strength of steel hardened and tempered at 500°C in dependence on arithmetic average distance between submicroscopic oxide impurities are presented in Fig. 5, regression equation and correlation coefficient r at (12).

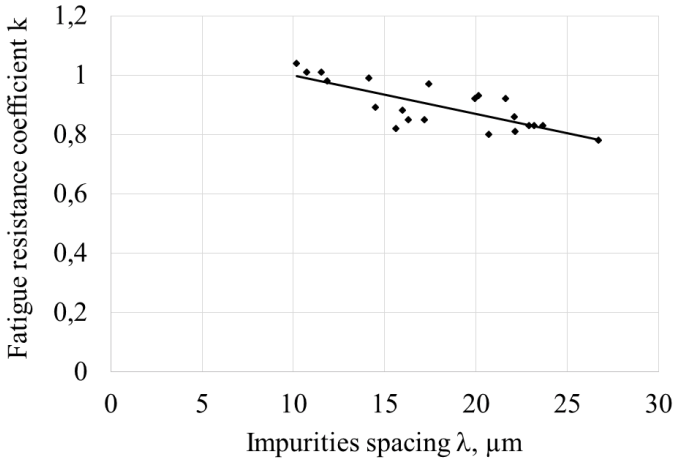

Fig. 5. Fatigue resistance coefficient k of steel hardened and tempered at 500°C subject to arithmetic average distance between submicroscopic oxide impurities (impurities spacing) λ

$$k_{(500)} = -0.0129\,\mathrm{l} + 1.1272 \quad \text{and} \quad r = 0.7768 \qquad (12)$$

Fatigue resistance coefficient k determined for bending fatigue strength of steel hardened and tempered at 600°C in dependence on arithmetic average distance between submicroscopic oxide impurities are presented in Fig. 6, regression equation and correlation coefficient r at (13).

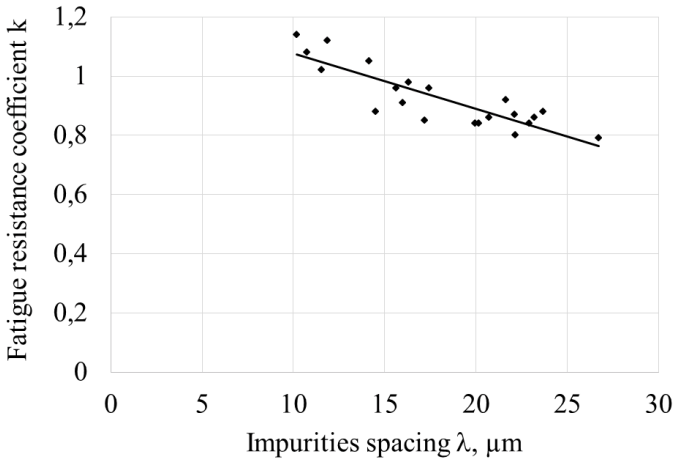

Fig. 6. Fatigue resistance coefficient k of steel hardened and tempered at 600°C subject to arithmetic average distance between submicroscopic oxide impurities (impurities spacing) λ

$$k_{(600)} = -0.0187\,\mathrm{l} + 1.263 \quad \text{and} \quad r = 0.8597 \qquad (13)$$

Fatigue resistance coefficient k determined for bending fatigue strength of steel hardened and tempered at all tempered temperatures in depends of arithmetic average distance between submicroscopic oxide impurities are presented in Fig. 7, regression equation and correlation coefficient r at (14).

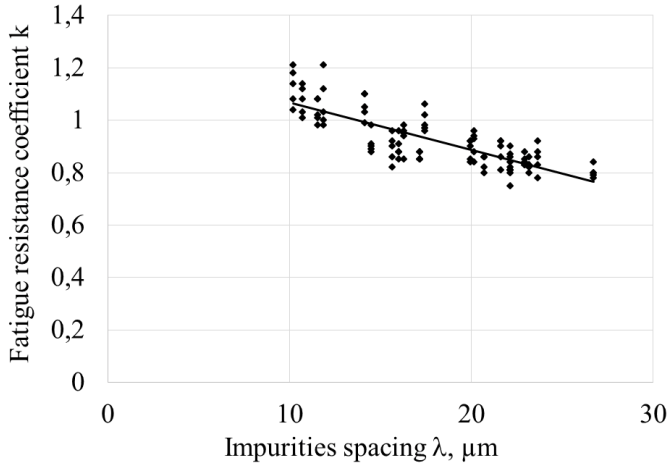

Fig. 7. Fatigue resistance coefficient k of steel hardened and tempered at all tempered temperatures subject to arithmetic average distance between submicroscopic oxide impurities (impurities spacing) λ

$$k = -0.0181\,l + 1.249 \quad \text{and} \quad r = 0.8098 \qquad (14)$$

Statistical parameters representing the results of the experiment are presented in Table 2.

TABLE 2

Statistical parameters representing the results of the experiment

t_{temp}, °C	$\bar{k}$	s_k	λ	s_λ, %
200	0.96	0.127	18.04	4.685
300	0.90	0.086		
400	0.93	0.118		
500	0.90	0.079		
600	0.926	0.104		

Parameters representing mathematical models and correlation coefficients are presented in Table 3.

The coefficient in equation (3) for different tempering temperatures and different microstructures (Table 3) is proportional to the arithmetic mean of its experimentally determined value (Table 2).

TABLE 3

Parameters representing mathematical models (4) and correlation coefficients (5)

Tempering temperature °C	Regression coefficient a (4)	Regression coefficient b (4)	Correlation coefficient r	Degree of dissipation k around regression line δ (6)	$t_{\alpha=0.05}$ calculated by (5)	$t_{\alpha=0.05}$ from Student's distribution for $p = (n-2)$
200	–0.0231	1.3737	0.8650	0.1275	7.514	2.093
300	–0.0161	1.193	0.8926	0.0776	8.630	
400	–0.0200	1.2878	0.8059	0.1397	5.933	
500	–0.0129	1.1272	0.7768	0.0995	5.377	
600	–0.0187	1.263	0.8597	0.1062	7.336	
all	–0.0181	1.249	0.8098	0.1232	14.008	1.983

all – arithmetic means of the analyzed parameters at all tempering temperatures.

4. Conclusions

The results of the study indicate that fatigue resistance coefficient k, represented by fatigue strength during rotary bending, is correlated with the relative volume of non-metallic inclusions measuring up to 2 µm. The presence of statistically significant correlations was verified by Student's t-test.

The value of distance between submicroscopic oxide impurities (impurities spacing) λ decreased as the number of inclusions increased (Fig. 1), which is a natural process. At the same time, a high correlation coefficient ($r = 0.95$) confirms that the equation is statistically significant and that the tests were conducted correctly.

A negative correlation coefficient describing the relationships in Figures 2-7 (Table 3) indicates that the fatigue resistance coefficient k decreases with an increase in impurities spacing λ.

The distance between submicroscopic non-metallic inclusions λ was inversely proportional to the value of fatigue resistance coefficient k. The above suggests that an increase in the number of submicroscopic inclusions in structural steel increases the value of k.

An analysis of regression coefficients and dissipation fatigue resistance coefficients k indicates that changes in coefficients k as a function of impurities spacing λ can be described with satisfactory accuracy by a single equation (14) at all tempering temperatures.

REFERENCES

[1] J. Szala, Assessment of Fatigue Life of Machine Elements Under Random Loads and Programmatic. Bydgoszcz University of Technology and Agriculture, Bydgoszcz 1980 (in Polish).
[2] W. Wołczyński, Mathematical Modeling of the Microstructure of Large Steel Ingots, Entry 196 [in:] The Encyclopedia of Iron, Steel, and Their Alloys, Eds. Taylor & Francis Group, New York-USA, 2015 (in print). DOI: 10.1081/E-EISA-120053685.
[3] A. Warhadpande, B. Jalalahmadi, T. Slack, F. Sadeghi, Int J Fatigue **32** 685 (2010).
[4] Guide engineer. Mechanic. Scientific and Technical Publishing Warsaw 1970 (in Polish).
[5] J. Kloch, B. Billia, T. Okane, T. Umeda, W. Wołczyński, Mater Sci Forum, **329/330**, 31 (2000).
[6] T. Himemiya, W. Wołczyński, Mater Trans **43**, 2890 (2002).
[7] W. Wołczyński, E. Guzik, B. Kania, W. Wajda, Archives of Foundry Engineering **9**, 254 (2009).
[8] W. Wołczyński, E. Guzik, W. Wajda, D. Jędrzejczyk, B. Kania, M. Kostrzewa, Arch Metall Mater **57**, 105 (2012).
[9] W. Wołczyński, W. Wajda, E. Guzik, Sol St Phen **197**, 174 (2013).
[10] T. Hongand, T. Debroy, Metall Mater Trans B **34B**, 267 (2003).
[11] S. Kimura, Y. Nabeshima, K. Nakajima, S. Mizoguchi, Mater Trans B **31B,** 1013 (2000).
[12] E.A. Chichkarev, Metallurgist, **53**, 728 (2009).
[13] T. Lipiński, A. Wach, in: 23rd International Conference on Metallurgy and Materials METAL 2014, TANGER Ltd. Ostrava 738 (2014).
[14] T. Lipiński, A. Wach, Sol St Phenom **223**, 46 (2015).
[15] T. Lipiński, A. Wach, Archives of Foundry Engineering **10** (2), 79 (2010).
[16] T. Lipiński, A. Wach,. Archives of Foundry Engineering **12** (2), 55 (2012).
[17] M.G. Hebsur, K.P. Abracham, V.V. Prasad, Eng Fract Mech **13** (4), 851 (1980).
[18] W. Wołczyński, J. Kloch, Mater Sci Forum, **329/330**, 345 (2000).
[19] W. Wołczyński, M. Bobadilla, A. Dytkowicz, Arch Metall Mater **45**, 303 (2000).
[20] J. Kowalski, J. Pstruś, S. Pawlak, M. Kostrzewa, R. Martynowski, W. Wołczyński, Arch Metall Mater **56**, 1029 (2011).
[21] T. Cornelius, K. Birger, I. Nils-Gunnar, Mater Trans A **37A**, 2995 (2006)
[22] Y. Hai–Liang, L. Xiang–Hua, B. Hong-Yun, Ch. Li-Qing, J Mater Process Tech **209**, 455 (2009).
[23] W. Wołczyński, Defect Diffus Forum **272**, 123 (2007).
[24] W. Wołczyński, Arch Metall Mater **62**, (2015) (in print).
[25] Y. Murakami, M. Endo, Int J Fatigue **16** (3), 163 (1994).
[26] T. Lis, Metall Foundry Eng **1 (**28), 29 (2002).
[27] T. Lipiński, A. Wach, Archives of Foundry Engineering **10** (Special Issue 4), 45 (2010).
[28] T. Lipiński, A. Wach, Arch Metall Mater **60** (1), 65 (2015).
[29] V.S. Gulyakov, A.S. Vusikhis, D.Z. Kudinov, Steel Transl **42** (11), 781 (2012).
[30] D. Spriestersbach, P. Grad, E. Kerscher, Int J Fatigue **64**, 114 (2014).
[31] S. Beretta, Y. Murakami, Mater Trans B **32B**, 517 (2001).
[32] J.M. Hang, S.X. Li, Z.G. Yang, G.Y. Li, W.J. Hui, Y.Q. Weng, Int J Fatigue **29** (2007).
[33] S. Maropoulos, N. Ridley, Mater Sci Eng A **384**, 64 (2004).
[34] Y. Murakami, S. Kodama, S. Konuma, Int J Fatigue **11** (5), 291 (1989).
[35] Z.G. Yang, S.X. Li, Y.D. Li, Y.B. Liu, W.J. Hui, Y.Q. Weng, Mater Sci Eng A **527**, 559 (2010).
[36] J. Ryś, Stereology of materials, Fotobit Design, Krakow 1995 (in Polish).

Received: 20 April 2015